

# Physical and optical properties of Ce:YAG nanophosphors and transparent ceramics and observation of novel luminescence phenomenon

S. AGARWAL,<sup>1</sup> M. S. HASEMAN,<sup>2</sup> A. KHAMEHCHI,<sup>3</sup> P. SAADATKIA,<sup>1</sup>  
D. J. WINARSKI,<sup>1</sup> AND F. A. SELIM<sup>1,2,\*</sup>

<sup>1</sup>Center for Photochemical Sciences, Bowling Green State University, Bowling Green, OH 43403, USA

<sup>2</sup>Department of Physics and Astronomy, Bowling Green State University, Bowling Green, OH 43403, USA

<sup>3</sup>Department of Physics and Astronomy, Washington State University, Pullman, WA 99164, USA

\*[faselim@bgsu.edu](mailto:faselim@bgsu.edu)

**Abstract:** Ce doped yttrium aluminum garnet (Ce:YAG) is an important photonic material that is used as a yellow phosphor for white light emitting diodes. In this work, the physical and optical properties of Ce:YAG nanophosphors are investigated and the effects of high-temperature thermal treatments and annealing atmospheres on the particle size and luminescence intensity are discussed. Furthermore, photo-luminescence (PL) was measured as a function of temperature and compared with PL from Ce:YAG single crystals and transparent ceramics to understand the mechanism of luminescence decay with temperature. While the characteristics of PL emission as a function of temperature for single crystals and NPs are similar and follow common decay trends, Ce:YAG transparent ceramics exhibit an interesting unusual increase in PL with temperature. We explained this unique novel behavior by a 4-step mechanism involving localized states in the band gap, and provided evidence from thermo-luminescence measurements to support this interpretation. The work reveals a new luminescence phenomenon arising from the overlap of PL and TL emissions; this phenomenon is most likely characteristic of transparent ceramics.

© 2017 Optical Society of America

**OCIS codes:** (300.2140) Emission; (300.6280) Spectroscopy, fluorescence and luminescence; (160.4236) Nanomaterials; (160.5690) Rare-earth-doped materials; (160.2220) Defect-center materials; (160.2540) Fluorescent and luminescent materials.

## References and links

1. W. Chewpraditkul, L. Swiderski, M. Moszynski, T. Szczesniak, A. Syntfeld-Kazuch, C. Wanarak, and P. Limsuwan, "Comparative studies of  $\text{Lu}_3\text{Al}_5\text{O}_{12}$ : Ce and  $\text{Y}_3\text{Al}_5\text{O}_{12}$ : Ce scintillators for gamma-ray detection," *Phys. Status Solidi., A Appl. Mater. Sci.* **206**(11), 2599–2605 (2009).
2. C. R. Varney, S. M. Reda, D. T. Mackay, M. C. Rowe, and F. A. Selim, "Strong visible and near infrared luminescence in undoped YAG single crystals," *AIP Adv.* **1**(4), 042170 (2011).
3. J. Dong, A. Shirakawa, K. Ueda, H. Yagi, T. Yanagitani, and A. A. Kaminskii, "Efficient  $\text{Yb}_3$ :  $\text{Y}_3\text{Al}_5\text{O}_{12}$  ceramic microchip lasers," *Appl. Phys. Lett.* **89**(9), 091114 (2006).
4. J. Huie, R. Gentilman and T. Stefanik, "Domestically produced ceramic YAG laser gain material for high power SSLs," *Proc. SPIE* **6552**, 65520B (2007).
5. A. Ikesue, T. Kinoshita, K. Kamata, and K. Yoshida, "Fabrication and optical properties of high-Performance polycrystalline Nd: YAG ceramics for solid-State lasers," *J. Am. Ceram. Soc.* **78**(4), 1033–1040 (1995).
6. E. Pawlowski, M. Kluge, Y. Menke, U. Peuchert, A. Engel, Y. L. Aung, A. Ikesue, K. Beil, R. Peters, H. Keuhn, K. Petermann, and P. Heist, "Yb: YAG composite ceramic laser," *Proc. SPIE* **7578**, 1–8 (2010).
7. A. Sennaroglu, C. R. Pollock, H. Nathel, J. Mass, J. Burlich, S. Margraf, and R. Dieckmann, "New  $\text{Cr}_4$  laser materials for the near infrared," *Proceedings of SPIE, (SPIE. Digital Library)* **2216**, 110–122 (1994).
8. X. Chen, H. Qin, X. Wang, C. Yang, J. Jiang, and H. Jiang, "Sintering and characterization of  $\text{Gd}_3\text{Al}_3\text{Ga}_2\text{O}_{12}/\text{Y}_3\text{Al}_5\text{O}_{12}$  layered composite scintillation ceramic," *J. Eur. Ceram. Soc.* **36**(10), 2587–2591 (2016).
9. E. Mihóková, M. Nikla, J. A. Mareš, A. Beitlerová, A. Vedda, K. Nejezchleb, K. Blažek, and C. D' Ambrosio, "Luminescence and scintillation properties of YAG: Ce single crystal and optical ceramics," *J. Lumin.* **126**(1), 77–80 (2007).

10. S. Chung, S. Chen, K. Wang, and C. Siao, "Promotion of solid-state lighting for ZnCdSe quantum dot modified-YAG-based white light-emitting diodes," *RSC Advances* **6**(57), 51989–51996 (2016).
11. N. Narendran, Y. Gu, J. Freyssinier, H. Yu, and L. Deng, "Solid-state lighting: Failure analysis of white LEDs," *J. Cryst. Growth* **268**(3-4), 449–456 (2004).
12. P. Yadav, C. Joshi, and S. Moharil, "Combustion synthesis of multicomponent ceramic phosphors for solid state lighting," *Int. J. Self-Propag. High-Temp. Synth.* **21**(1), 32–37 (2012).
13. J. Cheng, K. Qi, Q. Wang, and J. Wan, "Kind of electrovacuo glass in a YAG display tube," *Proceedings of SPIE, (SPIE. Digital Library)* **3560**, 227–232 (1998).
14. K. Ohno and T. Abe, "Bright green phosphor,  $Y_3Al_{5-x}Ga_xO_{12}$ : Tb, for projection CRT," *J. Electrochem. Soc.* **134**(8), 2072–2076 (1987).
15. T. Yanagida, H. Takahashi, T. Ito, D. Kasama, T. Enoto, M. Sato, S. Hirakuri, M. Kokubun, K. Makishima, T. Yanagitani, H. Yagi, T. Shigeta, and T. Ito, "Evaluation of Properties of YAG (Ce) Ceramic Scintillators," *IEEE Trans. Nucl. Sci.* **52**(5), 1836–1841 (2005).
16. S. Chen, H. Wei, C. L. Melcher, and Y. Wu, "Spectroscopic properties of transparent  $Y_3Al_5O_{12}$ : Eu ceramics," *Opt. Mater. Express* **3**(12), 2022–2027 (2013).
17. M. Gong, X. Liang, Y. Wang, H. Xu, L. Zhang, and W. Xiang, "Novel synthesis and optical characterization of phosphor-converted WLED employing Ce: YAG-doped glass," *J. Alloys Compd.* **664**, 125–132 (2016).
18. D. S. Kong, M. J. Kim, H. J. Song, I. S. Cho, S. Jeong, H. Shin, S. Lee, and H. S. Jung, "Fine tuning of emission property of white light-emitting diodes by quantum-dot-coating on YAG: Ce nanophosphors," *Appl. Surf. Sci.* **379**, 467–473 (2016).
19. Z. Lin, H. Lin, J. Xu, F. Huang, H. Chen, B. Wang, and Y. Wang, "Highly thermal-stable warm w-LED based on Ce: YAG PiG stacked with a red phosphor layer," *J. Alloys Compd.* **649**, 661–665 (2015).
20. G. Liu, Z. Zhou, Y. Shi, Q. Liu, J. Wan, and Y. Pan, "Ce: YAG transparent ceramics for applications of high power LEDs: Thickness effects and high temperature performance," *Mater. Lett.* **139**, 480–482 (2015).
21. L. Guerbous and A. Boukerika, "Nanomaterial host bands effect on the photoluminescence properties of Ce-doped YAG nanophosphor synthesized by sol-gel method," *J. Nanomater.* **2015**, 1–10 (2015).
22. X. He, X. Liu, R. Li, B. Yang, K. Yu, M. Zeng, and R. Yu, "Effects of local structure of Ce(3+) ions on luminescent properties of  $Y_3Al_5O_{12}$ :Ce nanoparticles," *Sci. Rep.* **6**, 22238 (2016).
23. K. J. Rajan and S. V. Manorama, "Formation of hierarchical macro porous YAlO: Ce multifunctional nanophosphors," *J. Appl. Phys.* **119**(11), 114902 (2016).
24. Y. Cho, Y. Huh, C. R. Park, and Y. R. Do, "Preparation with laser ablation and photoluminescence of  $Y_3Al_5O_{12}$ : Ce nanophosphors," *Electron. Mater. Lett.* **10**(2), 461–465 (2014).
25. J. L. Wu, G. Gundiah, and A. Cheetham, "Structure–property correlations in Ce-doped garnet phosphors for use in solid state lighting," *Chem. Phys. Lett.* **441**(4-6), 250–254 (2007).
26. D. A. Steigerwald, J. C. Bhat, D. Collins, R. M. Fletcher, M. O. Holcomb, M. J. Ludowise, P. S. Martin, and S. L. Rudaz, "Illumination with solid state lighting technology," *IEEE J. Sel. Top. Quantum Electron.* **8**(2), 310–320 (2002).
27. E. Zych, C. Brecher, and H. Lingertat, "Scintillation properties of YAG: Ce optical ceramics," *Mater. Sci. Forum* **239-241**, 257–260 (1997).
28. J. McKittrick, L. Shea, C. Bacalski, and E. Bosze, "The influence of processing parameters on luminescent oxides produced by combustion synthesis," *Displays* **19**(4), 169–172 (1999).
29. B. Sundarakannan and M. Kottaisamy, "Sol-gel derived flux assisted synthesis of fine particles YAG: Ce<sup>3+</sup> phosphor for remote phosphor converted white light emitting diodes," *Mater. Res. Bull.* **74**, 485–490 (2016).
30. L. Wang, F. Zhao, M. Zhang, T. Hou, Z. Li, and H. Huang, "Preparation and photoluminescence properties of YAG: Ce<sup>3+</sup> phosphors by a series of amines assisted co-precipitation method," *J. Alloys Compd.* **661**, 148–154 (2016).
31. T. Ogi, A. B. D. Nandiyanto, W. Wang, F. Iskandar, and K. Okuyama, "Direct synthesis of spherical YAG: Ce phosphor from precursor solution containing polymer and urea," *Chem. Eng. J.* **210**, 461–466 (2012).
32. F. A. Selim, A. Khamehchi, D. J. Winarski, and S. Agarwal, "Synthesis and characterization of Ce:YAG nanophosphors and ceramics," *Opt. Mater. Express* **6**(12), 3704–3715 (2016).
33. C. Yang, G. Gu, X. Zhao, X. Liang, and W. Xiang, "The growth and luminescence properties of  $Y_3Al_5O_{12}$ : Ce<sup>3+</sup> single crystal by doping Gd<sup>3+</sup> for W-LEDs," *Mater. Lett.* **170**, 58–61 (2016).
34. J. Ji, L. A. Boatner, and F. A. Selim, "Donor characterization in ZnO by thermally stimulated luminescence," *Appl. Phys. Lett.* **105**(4), 041102 (2014).
35. D. J. Winarski, C. Persson, and F. A. Selim, "Hydrogen in insulating  $Y_3Al_5O_{12}$  strongly narrows the energy gap," *Appl. Phys. Lett.* **105**(22), 221110 (2014).
36. S. M. Reda, C. Varney, and F. A. Selim, "Radio-luminescence and absence of trapping defects in Nd-doped YAG single crystals," *Results Phys.* **2**, 123–126 (2012).
37. C. H. Lu, H. C. Hong, and R. Jagannathan, "Sol-gel synthesis and photo luminescent properties of cerium-ion doped yttrium aluminum garnet powders," *J. Mater. Chem.* **12**(8), 2525–2530 (2002).
38. P. Husband, I. Bartošová, V. Slugeň, and F. A. Selim, "Positron annihilation in transparent ceramics," *J. Phys. Conf. Ser.* **674**, 012013 (2016).
39. S. Arjoca, E. G. Villora, D. Inomata, K. Aoki, Y. Sugahara, and K. Shimamura, "Temperature dependence of Ce: YAG single-crystal phosphors for high-brightness white LEDs/LDs," *Mater. Res. Express* **2**(5), 055503 (2015).

40. E. Zycha and C. Brecher, "Temperature dependence of Ce-emission kinetics in YAG: Ce optical ceramic," *J. Alloys Compd.* **300-301**, 495–499 (2000).
41. V. Bachmann, C. Ronda, and A. Meijerink, "Temperature Quenching of Yellow Ce<sup>3+</sup> Luminescence in YAG: Ce," *Chem. Mater.* **21**(10), 2077–2084 (2009).
42. D. J. Robbins, "The Effects of Crystal Field and Temperature on the Photoluminescence Excitation Efficiency of Cd + in YAG," *J. Electrochem. Soc.* **126**(1550), 9 (1979).
43. D. T. Mackay, C. R. Varney, J. Buscher, and F. A. Selim, "Study of exciton dynamics in garnets by low temperature Thermo-luminescence," *J. Appl. Phys.* **112**(2), 023522 (2012).
44. C.R. Varney, D.T. Mackay, A. Pratt, S.M. Reda, and F.A. Selim, "Energy levels of exciton traps in YAG single crystals," *J. Appl. Phys.* **111**, 063505 (2012).
45. F. A. Selim, C. R. Varney, M. C. Tarun, M. C. Rowe, G. S. Collins, and M. D. McCluskey, "Positron lifetime measurements of hydrogen passivation of cation vacancies in yttrium aluminum oxide garnets," *Phys. Rev. B* **88**(17), 174102 (2013).

## 1. Introduction

Yttrium Aluminum Garnet, Y<sub>3</sub>Al<sub>5</sub>O<sub>12</sub> (YAG) has been the subject of intense research efforts because of their wide use as detectors, laser host materials and phosphors [1–7]. In particular, a great deal of research has been conducted on doping and co-doping YAG with transition metals like Ce, Nd, Eu, Dy, Yb, Cr to investigate their effects on its optical properties [1–16]. Cerium-doped YAG (Ce: YAG) has received considerable attention because of its intense emission at 525 nm and its important role in converting blue emission to white light in InGaN light-emitting diodes [17–20]. Ce:YAG nanophosphors (NPs) may offer several advantages for white light emitting diodes (WLEDs) [21–26] because of their small size, less Ce segregation and simple preparation. The traditional solid state chemical methods used for the synthesis of conventional Ce:YAG ceramic powder require very high temperatures and prolonged mixing time, resulting in inhomogeneity and a large grain size of hundreds of microns [27,28]. Moreover, solid state methods induce high levels of defects which affect the optical properties and exciton dynamics. Wet chemical routes such as sol-gel methods have significantly reduced the temperature required for the formation of YAG phase, as well as reduced the mixing temperature which allows for better control of particle size and doping limit [22, 27–31]. In a recent paper we have reported on two sol-gel synthesis pathways for Ce:YAG nanophosphors and the role of complexing and polymerization agents [32].

In the current work we investigate the physical and optical properties of Ce:YAG NPs prepared by the sol gel method including particle size and photoluminescence, and the corresponding effects of annealing temperature and environment as well as compare NP emission with that of Ce:YAG transparent ceramics and single crystals and investigate their luminescent decay with temperature. The results presented here reveal how the luminescent properties of Ce:YAG NPs are strongly affected by annealing temperature and atmosphere. The temperature dependent photo-luminescence (PL) has not been well investigated and the thermal quenching of luminescence in Ce:YAG is not yet understood despite its importance in LED performance. In this work, we present a comprehensive study of temperature-dependent PL from 83 to 633 K for Ce:YAG NPs, single crystals (SC) and transparent ceramics, and report on a new optical behavior in the PL of Ce:YAG transparent ceramics. While we observe the usual temperature-dependent PL quenching for NP and SC, there is a significant difference in the PL spectra of Ce:YAG transparent ceramics, in which the luminescent intensity increases with increasing temperature, an unusual phenomenon which we ascribe to the presence of large populations of trap levels in the band gap and the contributions of thermally-stimulated luminescence in the PL spectra. We are not aware of any reports on similar phenomenon in PL temperature dependence studies.

## 2. Experimental details

### 2.1 Material preparation

Ce: YAG nanophosphors were prepared using the sol-gel method as described in our recent work [30] using yttrium nitrate, aluminum nitrate and cerium nitrate mixed in a stoichiometric

amount (5% Ce- doped) and dissolved in distilled water. Urea and poly vinyl alcohol were used as complexing and polymerizing agents respectively. The solution was heated for 2 h at 150°C, dried and calcined at 600°C for a few hours. Annealing was done in a GSL-1700X series tube furnace in air at various temperatures from 600 to 1500°C, each for 18 hours. YAG transparent ceramics doped with 0.5% Ce were obtained from Baikowski/ Konoshima Inc. and Single crystals doped with 0.1% Ce were grown by the Czochralski method in Crytur Inc [32]. under an atmosphere of 40% hydrogen in argon. The size of each sample is 1 cm diameter and 1 mm thickness.

### 2.2 Structural and luminescence characterization

Structural characterization of the Ce:YAG samples was carried out via X-ray diffraction (XRD) measurements. The diffraction intensity vs  $2\theta$  was recorded using a Rigaku diffractometer and the average grain size was calculated using the Scherer equation. Photoluminescence measurements were carried out using a blue LED (456 nm) as an excitation source and a monochromator to remove the tail at longer wavelengths. A BWTEK GlacierX spectrometer was used to record the luminescence emission versus wavelength spectra. For the temperature-dependent photo-luminescence measurements, we used a heating stage equipped with a specialized window that efficiently transmits UV and visible light. The temperature was controlled using an INSTRON Heat Stage Profile instrument. Thermoluminescence (TL) was recorded via a special spectrometer designed and constructed in-house, allowing for direct measurement of the luminescence as a function of both wavelength and temperature [34–36]. A 456 nm blue LED was used to irradiate each sample at  $-190^{\circ}\text{C}$  for 30 minutes. We used the same 456 nm LED for PL and TL measurements because we are interested to examine if TL would contribute to the temperature dependent PL spectra. After irradiation, the samples were linear-ramp heated to 400°C at a rate of 60°C /min and the corresponding luminescent spectrum was recorded from 200 to 800 nm using a charge-coupled device detector. TL measurements were carried out on Ce:YAG nanophosphors, transparent ceramics and single crystals under similar conditions. The excitation light was focused on a small area on the center of each sample to ensure the measurement of equal areas from single crystals, ceramics and NPs. No TL emission was observed from Ce:YAG nanophosphors or single crystals after irradiation with 456 nm light.

## 3. Results and discussions

Figure 1 shows the X-ray diffraction pattern of Ce: YAG NPs annealed at various temperatures ranging from 1000 to 1500°C. The formation of pure YAG phase is first seen at 1000°C, however, when the sample was annealed in the range of 600 to 900°C, XRD pattern revealed the absence of YAG phase. When the sample was annealed at higher temperatures of 1000- 1500°C, pure YAG phase was obtained, however, a minor peak indicating the presence of CeO<sub>2</sub> impurity phase at  $2\theta = 28$  degree was observed. The formation of CeO<sub>2</sub> phase can either be due to phase segregation or non-uniform mixing of the reactants [37].

Figure 2 illustrates the dependence of grain size on annealing temperature. At higher temperatures, the particle size tends to increase with annealing temperature due to grain growth. The figure also shows that the rate of increase is less from 1300 to 1500°C, however we cannot anneal above 1500°C to further investigate when it reaches saturation.

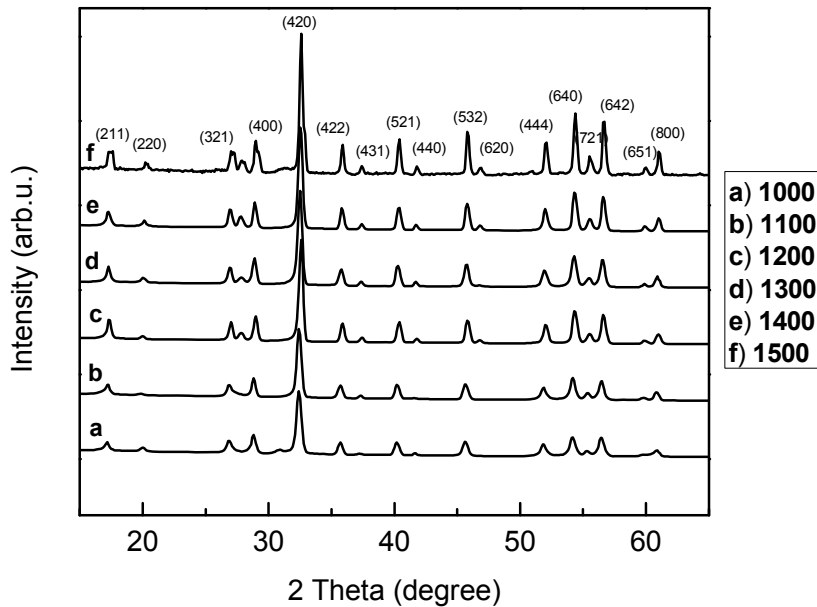


Fig. 1. XRD patterns of Ce:YAG nanophosphors annealed in various temperatures from 1000 to 1500°C. All YAG orientations are labelled on the graph.

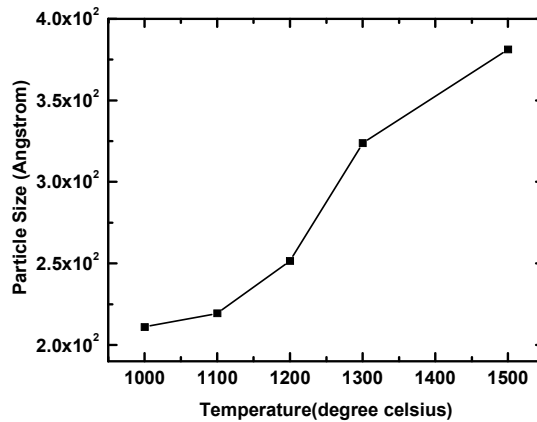


Fig. 2. Grain size of Ce:YAG nanophosphors annealed at various temperatures from 1000 to 1500°C.

Figure 3 displays the photo-luminescence (PL) emission spectrum of Ce:YAG NPs; the well-known emission at 525 nm results from the 5d to 4f transitions of  $\text{Ce}^{3+}$ . No PL was observed after annealing between 600 and 900°C which is consistent with the absence of YAG phase in the XRD patterns. It can be seen that PL intensity dramatically increases with annealing temperature in Fig. 3(a). There are a few factors that may be responsible for this increase: a) better incorporation of  $\text{Ce}^{3+}$  in the matrix, b) more efficient formation of YAG phase and c) decrease in surface defects possibly resulting from a lower surface area to volume ratio; as the particle size increases, the grain density and the subsequent number of surface defects decrease, on the opposite, lower annealing temperatures lead to smaller particle sizes, which in turn leads to a higher number of surface defects that may inhibit the transport of photons.  $\text{CeO}_2$  was the only impurity phase observed in the XRD of samples,

however  $Ce^{4+}$  (electronic configuration:  $4f^0$ ) in  $CeO_2$  does not have any optical transition in the green region and thus does not contribute to the PL emission intensity at all [37]. It is interesting to note that if we anneal CeYAG NPs at high temperatures in the presence of air, the process of oxidation is inevitable and some of the  $Ce^{3+}$  ions oxidize to  $Ce^{4+}$ . To verify this, Ce:YAG nanophosphor was annealed in air at  $1200^\circ C$  for 12 hours and then divided into three parts. One was left as-is, while the other two parts were separately re-annealed in relatively reduced atmospheres of 1) hydrogen, and 2) argon, each at  $1200^\circ C$  for 1 hour. Their PL spectra in Fig. 3(b) show that the PL intensity significantly increased after annealing in reducing atmospheres of  $H_2$  or Ar. The reason behind that is the reduction of  $Ce^{4+}$  to  $Ce^{3+}$  state, which is responsible for the green emission in YAG.

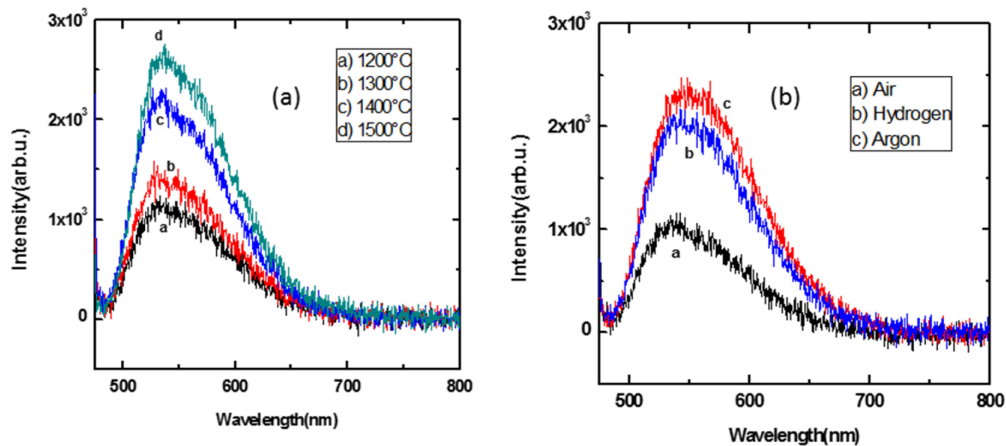


Fig. 3. PL intensity of Ce: YAG nanophosphors as a function of wavelength: (a) for different annealing temperatures, (b) for different annealing atmospheres.

Figure 4 compares the PL emission of Ce:YAG nanophosphor (annealed at  $1500^\circ C$ ) with Ce:YAG single crystal (SC) and transparent ceramics emission recorded under the same excitation conditions. It is interesting to note that the Ce:YAG NP prepared in this work is more efficient than SC and transparent ceramics despite the excellent transparency of the Ce:YAG transparent ceramic samples [38]. No significant peak shift is observed in nanophosphor ( $\lambda_{max} = 533nm$ ) compared to ceramics ( $\lambda_{max} = 532nm$ ) and single crystal ( $\lambda_{max} = 527nm$ ). The high intensity of PL emission in Ce:YAG NP can be explained due to high doping of Ce (5%) compared to (0.1%) in single crystal and (0.5%) in transparent ceramics. Both SC and transparent ceramics have been known to face strong Ce segregation and agglomeration when doped with high concentrations. One of the advantages of wet chemical method for phosphor preparation is that it allows higher doping. Figure 4 clearly demonstrates the high efficiency of the Ce:YAG NPs prepared in this work and its relevance to be used in the investigation of the luminescence characteristics of NPs.

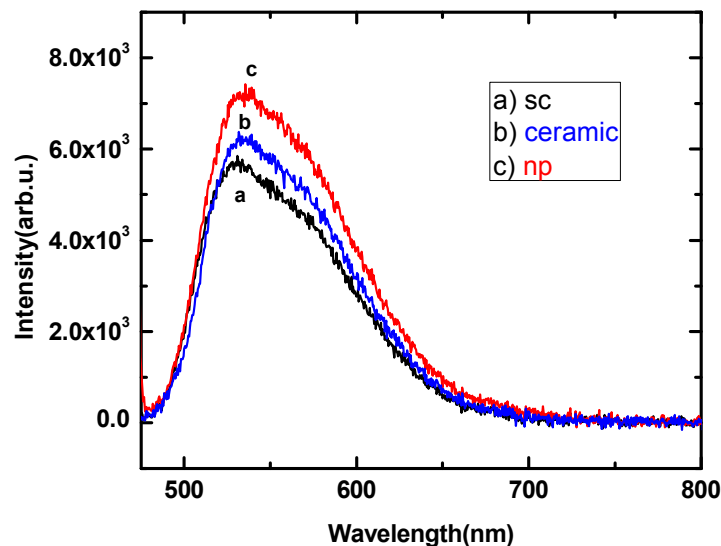


Fig. 4. PL emission intensity as a function of wavelength. The graph compares the emission of Ce: YAG NPs with single crystals and transparent ceramics.

A main drawback of phosphors is their luminescence quenching with little increase in temperature which limits their applications. Though many groups have tried to address the issue for bulk materials [39–42], much has to be done to utilize nanophosphors as a substitute emitter with excellent luminescence even at high temperatures. Up to now there is no significant data on luminescence quenching with increasing temperature in Ce:YAG nanophosphors. To address that and to obtain a better understanding for PL characteristics in Ce:YAG, PL spectra of Ce: YAG NPs (annealed at 1300°C) were recorded at various temperatures from 83 to 623 K as shown in Fig. 5(a). The spectra demonstrate intense emission at 83 K which gradually decreases with increasing temperature. However, Fig. 5(b) shows that even at a high temperature of 623 K, Ce:YAG NPs prepared in this work still emit low levels of light. At low temperatures, the emission band displays the well-known double band structure peaks as shown in Fig. 5(a) which broadens and appears as one peak at higher temperatures [41]. These double band peaks are the result of transitions from the lowest Stark level of the 5d excited state to the two Stark levels ( $2F_{5/2}$  and  $2F_{7/2}$ ) of the 4f ground state of  $Ce^{3+}$ .

The decrease of luminescence with increasing temperature is often observed in materials but an exact universal explanation has yet to be reported. It can be however related to the temperature dependence of the oscillator strength of a material. In Ce:YAG it is expected that  $2f_{5/2}$  level becomes thermally populated at higher temperatures which results in less absorption strength and in return gives less luminescence output. Also another possible reason for the decrease in luminescence is the energy migration to defects and non-radiative decay. PL emission spectra were recorded from 83 to 623 K at every 20 or 30 K interval, Fig. 5(a) includes only a handful of them for better display, while Fig. 5(c) displays the integrated peak area as a function of temperature measured from 83 to 623 K to give the overall picture. The graph reveals an interesting behavior. Instead of gradually quenching with the increase in temperature, PL intensity undergoes a little increase around 200 K, then decreases again.

To provide a deeper insight into the characteristics of PL emission intensity decrease with temperature, we carried out temperature-dependent PL measurements on Ce:YAG SC and transparent ceramics followed by thermo-luminescence (TL) spectroscopy. Figure 6 and Fig.

7 illustrate the temperature dependence of PL in SCs and transparent ceramics respectively. Single crystals and NPs share the same characteristics, including the slight increase at 200 K, and exhibit overall decay in luminescence with rising temperature while PL in Ce:YAG transparent ceramics manifests surprising behavior in which the luminescence intensity is not maximized at low temperatures; on the contrary it becomes very intense and broad in the 373-473 K temperature range before quenching.

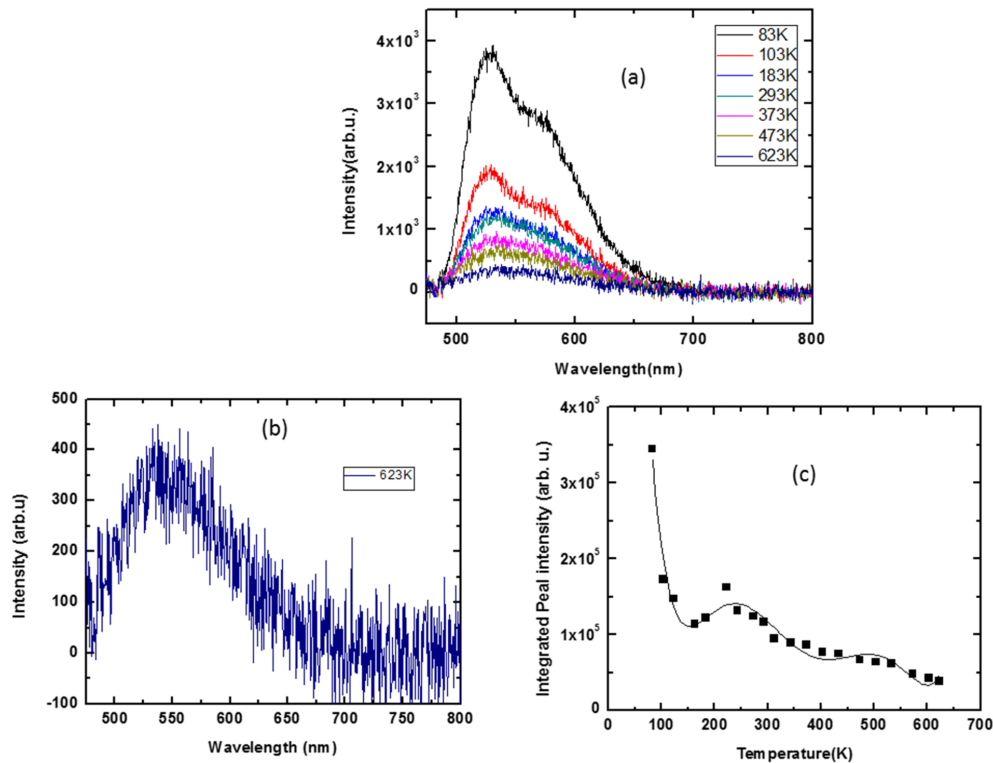


Fig. 5. a) Temperature dependent PL emission measurement of NP as a function of wavelength over temperature range of 83K-623K. b) PL emission intensity of NP at  $T = 623\text{K}$ . c) Integrated PL peak intensity as a function of temperature for NP. It shows that the luminescence intensity sharply decays with rising temperature up to 200 K where it undergoes a little increase, then decays again.

Our previous studies on TL have proved it to be an effective tool to investigate trap levels in semiconductors and dielectrics [43,44] and correlate them with many of the electronic properties of the materials. TL behavior in Ce:YAG may facilitate interpretation of the temperature dependence PL behavior reported in this work. In TL spectroscopy, materials are irradiated by high energy photons such as UV, x-ray or  $\gamma$ -rays to excite electrons from the valence band to the conduction band and to generate charge carriers. In the presence of defects, electrons and holes may become trapped. Subsequent heating then provides sufficient thermal energy for electron de-trapping, allowing for the transfer of energy to recombination centers leading to light emission. By recording the emission vs temperature and wavelength and constructing the glow curve, information about trap levels in the band gap can be obtained. Our interest in the current study is to investigate the possible presence of TL emission and its contribution to the PL intensity measured under 456 nm light. We therefore illuminated the samples with 456 nm light to populate electrons in the conduction band, at a temperature of 83K. No TL emission was detected in Ce:YAG NPs or single crystals, while a strong TL emission was measured in Ce:YAG transparent ceramics. Figure 8(a) and Fig. 8(b) display the TL contour plot and glow curve respectively. The glow curve was constructed by



integrating the emission over all wavelengths at each temperature. By comparing the TL glow curve in Fig. 8(b) with the PL emission in Fig. 7(b), we conclude that TL emission significantly contributes to the PL intensity and is responsible for the increase of PL with temperature. This conclusion is also consistent with the absence of TL emission in NPs and SCs and the decrease in their PL with temperature.

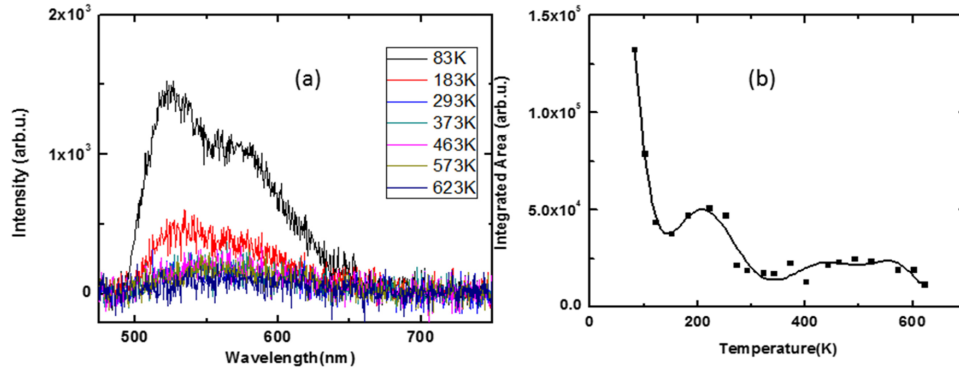


Fig. 6. a) Temperature dependent PL measurements of Ce:YAG single crystal. b) Integrated PL intensity of Ce:YAG single crystal as a function of temperature.

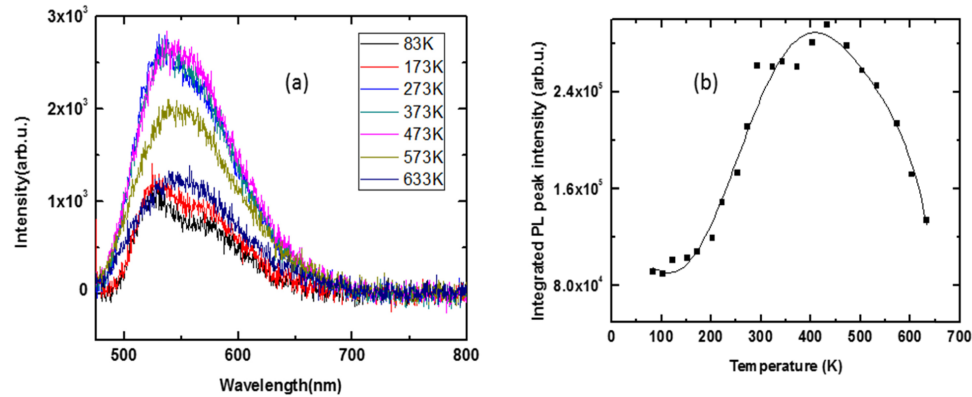


Fig. 7. a) Temperature dependent PL emission spectra of Ce:YAG transparent ceramics as a function of wavelength over a temperature range of 83 to 633 K. b) Integrated PL peak intensity of Ce:YAG transparent ceramics as a function of temperature.

The 456 nm (2.72 eV) light used for excitation in TL and PL is much lower than the band gap of YAG which is in the order of 6.5 eV and thus cannot excite electrons from the valence band to the conduction band. A defect center below the conduction band by 2.72 eV should be responsible for providing electrons to the conduction band while a separate defect center or impurity may act as an electron trap. From the analysis of TL glow curve we identified it as trap level of  $1.021 \pm 0.074$  eV below the conduction band. The detailed method of trap level calculations can be found in references [44]. From these calculations and by comparing emission in Fig. 7(b) and Fig. 8(b), we suggest a model as shown in Fig. 9 to explain the interesting behavior of PL increase with temperature. The model illustrates a four-step mechanism: a) excitation of an electron from a defect center to the conduction band, b) capture of the electron by a trap level of 1.02 eV in the band gap, c) thermal stimulation of the electrons from the trap, d) electron recombination in Ce atom emitting luminescence. No TL emission has been detected in NPs and SCs after excitation by 456 nm light. Accordingly, the small increase in PL around 200 K cannot be explained by this model; it is most likely a result

of thermal excitations of electrons from 4f to 5d levels during heating which then decays back and leads to a modest increase in PL intensity despite the contrary effect of the temperature dependence of the oscillator strength. Another possible scenario for the increase at 200 K could be the increase in the charge transfer due to higher mobility of the charge carriers, before it starts thermal quenching. We believe that the big difference between NP/SC and transparent ceramics is due to the nature and concentration of traps. The presence of voids in the grain boundaries of transparent ceramics provides an array of trap levels leading to this behavior. Previous positron annihilation spectroscopy measurements by one of the authors on YAG and Ce:YAG [38,45] have confirmed the presence of large voids only in transparent ceramics samples.

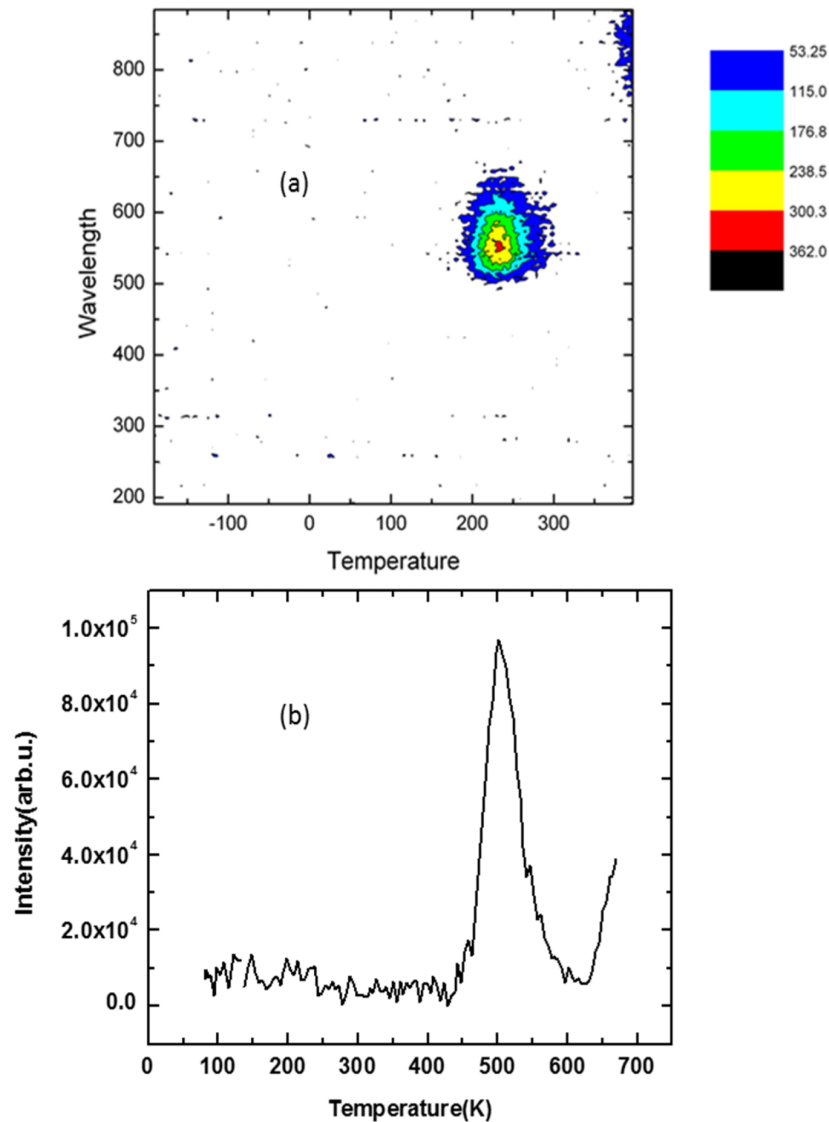


Fig. 8. a) Thermo-luminescence contour plot of Ce: YAG transparent ceramics as function of temperature and wavelength. Excitation was carried out using sub-band gap light of 456 nm (2.72 eV). b) Glow curve of TL emission of Ce: YAG transparent ceramics.

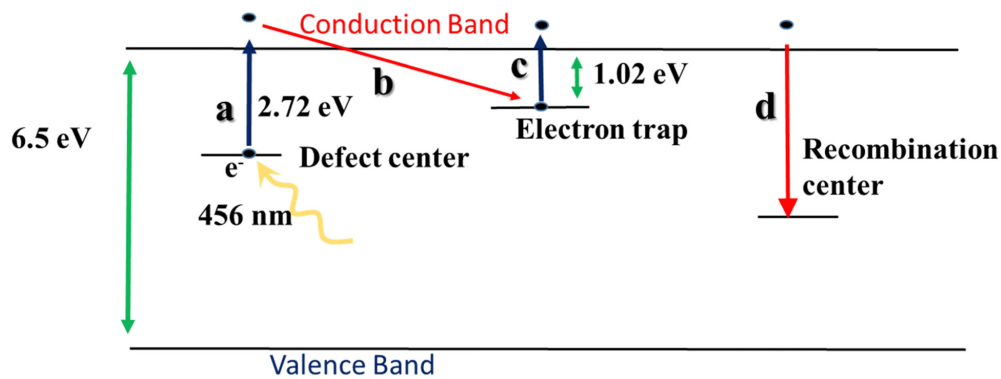


Fig. 9. Diagram illustrating the mechanism behind TL emission and its contribution to PL spectrum. a) Excitation of electron from defect center to the conduction band by 456 nm light, b) trapping of electron by another defect center, c) thermal stimulation, d) recombination of charge carriers and light emission.

#### 4. Conclusions

The physical and luminescence properties of Ce:YAG NPs and their dependence on annealing temperature and atmosphere were investigated. The measurements showed that Ce:YAG NPs prepared by simple sol-gel method are highly efficient phosphors. High-temperature annealing was found to increase the grain size and enhance the green luminescence while annealing in reducing atmospheres of Ar or H<sub>2</sub> significantly improved the emission. From temperature dependent PL measurements we showed similar PL temperature dependent dynamics for Ce:YAG NP and SC and revealed an interesting luminescence phenomenon in transparent ceramics due to the combination of TL and PL emissions, which leads to a large increase in luminescence with temperature, a phenomenon that has not been previously reported in any system. The presence of voids in transparent ceramic generates a large array of trap levels triggering this behavior; thus we suggest that this new luminescence phenomenon is characteristic of transparent ceramics.

#### Funding

We acknowledge receiving funds from the National Science Foundation under DMR 1359523 grant.